THE EUROPEAN
PHYSICAL JOURNAL
SPECIAL TOPICS

Regular Article

Alterations in brain connectivity due to plasticity and synaptic delay

E.L. Lameu[1,a], E.E.N. Macau[1,2], F.S. Borges[3], K.C. Iarosz[3], I.L. Caldas[3],
R.R. Borges[4], P.R. Protachevicz[5], R.L. Viana[6], and A.M. Batista[3,5,7]

[1] National Institute for Space Research, São José dos Campos, SP, Brazil
[2] Federal University of São Paulo, São José dos Campos, SP, Brazil
[3] Physics Institute, University of São Paulo, São Paulo, SP, Brazil
[4] Department of Mathematics, Federal Technological University of Paraná,
Ponta Grossa, PR, Brazil
[5] Science Post-Graduation, State University of Ponta Grossa, Ponta Grossa, PR,
Brazil
[6] Physics Department, Federal University of Paraná, Curitiba, PR, Brazil
[7] Department of Mathematics and Statistics, State University of Ponta Grossa,
Ponta Grossa, PR, Brazil

Abstract. Brain plasticity refers to brain's ability to change neuronal
connections, as a result of environmental stimuli, new experiences, or
damage. In this work, we study the effects of the synaptic delay on
both the coupling strengths and synchronization in a neuronal net-
work with synaptic plasticity. We build a network of Hodgkin–Huxley
neurons, where the plasticity is given by the Hebbian rules. We ver-
ify that without time delay the synapses become regulated by both
the nature (excitatory or inhibitory) and the frequency of the presy-
naptic and postsynaptic neuron. A presynaptic excitatory (inhibitory)
neuron with higher (lower) frequency enhances the synaptic strength if
the postsynaptic excitatory (inhibitory) neuron has lower (higher) fre-
quency. When the delay is increased the network presents a non-trivial
topology. Regarding the synchronization, only for small values of the
synaptic delay this phenomenon is observed.

1 Introduction

Neuroplasticity, also known as brain plasticity, refers to brain's ability to change neu-
ronal connections, as a result of environmental stimuli, new experiences, or damage
[1]. The brain plasticity can be functional or structural. The functional plasticity
occurs when functions are moved from a damaged to other undamaged areas, and
structural plasticity is associated with changes in the physical structure [2]. On this
regard, Borges et al. [3,4] studied the effects of the spike timing-dependent plasticity
(STDP) on the neuronal synchronization. They observed that the transition between
desynchronized and synchronized states depends on the external perturbation level

[a] e-mail: ewandson.ll@gmail.com

and the neuronal architecture. It is know that neuronal synchronization is important in information binding [5] and cognitive functions [6]. Nevertheless, synchronization can be related to brain disorders such as Parkinson's disease [7] and seizures [8]. This way, there have been many researches about not only neuronal synchronization [9], but also suppression of synchronous behavior [10].

We focus here on the effects of the synaptic delay on a neuronal network with STDP. Information transmission delay is inherent due to both the delays in synaptic transmission and the finite propagation velocities in the conduction of signals [11]. Hao et al. [12] studied synchronization transitions in a modified Hodgkin–Huxley neuronal network with time delay. They found multiple synchronization transitions when the time delay is considered.

Experimental evidence of neuroplasticity was provide by Lashely in 1923 [13]. He identified high evidence of changes in neural pathways by means of experiments on rhesus monkeys. More significant evidence began to be observed in the 1960s. In 1964, Diamond et al. [14,15] published research about neuroplasticity, which is considered as the first evidence of anatomical brain plasticity. Bach-y-Rita [16] created a machine that helped blind people not only to distinguish objects, but also to read. In 1949, the neuropsychologist Donald Olding Hebb [17] wrote a book entitled "The organization of behavior", where he proposed that neurons which fire together, also wire together. The Hebbian plasticity model led to a spike timing-dependent plasticity (STDP). The STDP function for excitatory and inhibitory synapses were showed by Bi and Poo [18] and Haas et al. [19], respectively.

In this work, our results suggest that alterations in the synchronization and connectivity in a plastic network depend on the synaptic delay. Without time delay synchronization is promoted and the network's topology becomes strongly structured, where the synapse that link the pre and postsynaptic neuron becomes enhanced or not depending on the nature of the neuron synaptic propensity (excitatory or not) and the neuron frequency. When time-delay is turned on the networks topology becomes highly non-trivial, and leading to a weak form of synchronization. We consider a Hodgkin–Huxley neuronal network with inhibitory and excitatory neurons. The Hodgkin–Huxley model [20] was proposed in 1952, and it is given by coupled differential equations that explains the ionic mechanisms.

This paper is organized as follows: Section 2 introduces the Hodgkin–Huxley neural network with synaptic delay. In Section 3, we introduce the synaptic plasticity. In Section 4, we show our results about synaptic weights and neuronal synchronization. In Section 5, we draw the conclusions.

2 Hodgkin–Huxley neural network with synaptic delay

In the neuronal network we consider as local dynamics the neuron model proposed by Hodgkin and Huxley in 1952 [20]. The individual dynamics of each neuron in the network is given by

$$
C\dot{V}_i = I_i - g_{\mathrm{K}} n_i^4 (V_i - E_{\mathrm{K}}) - g_{\mathrm{Na}} m_i^3 h_i (V_i - E_{\mathrm{Na}})
$$
$$
- g_L (V_i - E_{\mathrm{L}}) + \frac{(V_r^{\mathrm{Exc}} - V_i)}{\omega_{\mathrm{Exc}}} \sum_{j=1}^{N_{\mathrm{Exc}}} \varepsilon_{ij} f_j(t)
$$
$$
+ \frac{(V_r^{\mathrm{Inhib}} - V_i)}{\omega_{\mathrm{Inhib}}} \sum_{j=1}^{N_{\mathrm{Inhib}}} \sigma_{ij} f_j(t), \tag{1}
$$
$$
\dot{n}_i = \alpha_{n_i}(V_i)(1 - n_i) - \beta_{n_i}(V_i) n_i, \tag{2}
$$

$$\dot{m}_i = \alpha_{m_i}(V_i)(1 - m_i) - \beta_{m_i}(V_i)m_i, \tag{3}$$

$$\dot{h}_i = \alpha_{h_i}(V_i)(1 - h_i) - \beta_{h_i}(V_i)h_i, \tag{4}$$

where C (μF/cm^2) is the membrane capacitance and V_i (mV) is the membrane potential of neuron i ($i = 1, \ldots, N$). I_i represents a constant current density that is randomly distributed in the interval $[9.0; 10.0]$, ω_{Exc} (excitatory) and ω_{Inhib} (inhibitory) are the average degree connectivities, ε_{ij} and σ_{ij} are the excitatory and inhibitory coupling strengths from the presynaptic neuron j to the postsynaptic neuron i. N_{Exc} and N_{Inhib} are the number of excitatory and inhibitory neurons, respectively. The parameters g_K, g_{Na} and g_L are the conductances of the potassium, sodium and leak ion channels, respectively. E_K, E_{Na} and E_L are the reversal potentials for these ion channels. The functions $m(V_i)$ and $n(V_i)$ represent the activation for sodium and potassium, respectively. $h(V_i)$ is the function for the inactivation of sodium. The functions α_n, β_n, α_m, β_m, α_h, β_n are given by

$$\alpha_n(v) = \frac{0.01v + 0.55}{1 - \exp(-0.1v - 5.5)}, \tag{5}$$

$$\beta_n(v) = 0.125 \exp\left(\frac{-v - 65}{80}\right), \tag{6}$$

$$\alpha_m(v) = \frac{0.1v + 4}{1 - \exp(-0.1v - 4)}, \tag{7}$$

$$\beta_m(v) = 4 \exp\left(\frac{-v - 65}{18}\right), \tag{8}$$

$$\alpha_h(v) = 0.07 \exp\left(\frac{-v - 65}{20}\right), \tag{9}$$

$$\beta_h(v) = \frac{1}{1 + \exp(-0.1v - 3.5)}, \tag{10}$$

where $v = V/[mV]$. The neuron can present periodic spikings or single spike activity as a result of the variation of the external current density I_i (μA/cm^2). The frequency of the periodic spikes increases if the constant I_i increases.

In equation (1) the term $f_j(t)$ is a function which represents the strength of an effective synaptic (output) current and it is given by

$$f_j(t) = e^{\frac{-(t - t_j - \tau)}{\tau_s}}, \tag{11}$$

where τ_s is the synaptic time constant and t_j is the most recent firing instant of the neuron j. The parameter τ is the time delay and consequently the time that the current $f_j(t)$ spends to achieve the postsynaptic neuron [12]. Figures 1a and 1c show the time evolution of the action potential $V_j(t)$ for $\tau = 0$ and $\tau = 3$ ms, respectively. The action potential starts at -70 mV and when a stimulus is applied it spikes upward. After the peak potential, the action potential falls to the resting potential. In Figures 1b and 1d we calculate $f_j(t)$ for the respective Figures 1a and 1c. We see by means of the dashed green line that the transmission of the synaptic current to the postsynaptic is not instantaneous for $\tau = 3$ ms.

In our simulations, we consider $C = 1\,\mu$F/cm^2, $E_{\text{Na}} = 50$ mV, $E_{\text{K}} = -77$ mV, $E_{\text{L}} = -54.4$ mV, $g_{\text{Na}} = 120$ mS/cm^2, $g_{\text{K}} = 36$ mS/cm^2, $g_{\text{L}} = 0.3$ mS/cm^2 and $\tau_s = 2.728$ ms. The neurons are excitatorily coupled with a reversal potential $V_r^{\text{Exc}} = 20$ mV, and inhibitorily coupled with a reversal potential $V_r^{\text{Inhib}} = -75$ mV [4].
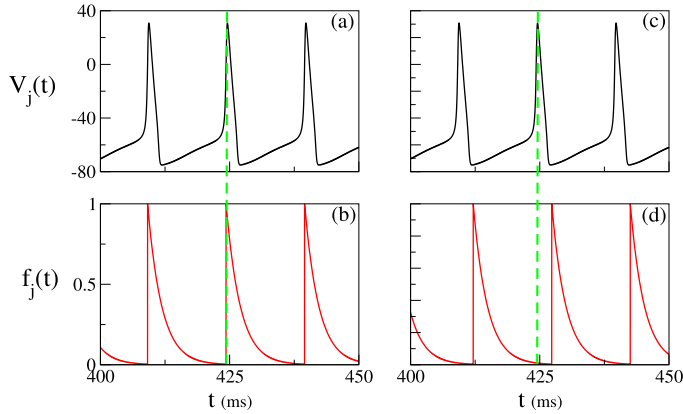
Fig. 1. Time evolution of the action potential $V_j(t)$ of a presynaptic neuron j and the respective synaptic current (output) $f_j(t)$ that achieves the postsynaptic neuron i. We consider $\tau = 0.0$ ms in (a) and (b), and $\tau = 3.0$ ms in (c) and (d).

3 Synaptic plasticity

Synaptic plasticity is the process that produces changes in the synaptic strength, namely it is the strengthening or weakening of synapses over time. In 1998, the neuroscientists Bi and Poo [18] characterized the dependence of the long-term potentiation and depression on the order and timing of pre and postsynaptic spikes, named spike time dependent plasticity (STDP). The plasticity dynamics is given by the update value of the synaptic weight $\Delta\Gamma$, and a mathematical definition of this function is given by [21]

$$\frac{d\Delta\Gamma(t)}{dt} = y(\Delta\Gamma, V, t). \tag{12}$$

Kalitzin and collaborators [21] showed that the function y depends on the membrane potential of the postsynaptic neuron, the activation of the synapse, and the thresholds for switching on long-term potentiation and the long-term depression. We consider an approximation of y in the linear form $y(\Delta\Gamma, t) = (a + c/t)\Delta\Gamma$ [4]. The function $\Delta\Gamma = bt^c \exp(at)$ is the solution of equation (12), where a, b, and c are constants. For $c = 0$, we obtain the update value for excitatory synapses $\Delta\varepsilon$ (eSTDP), and for $c \neq 0$, we find the update value for inhibitory synapses $\Delta\sigma$ (iSTDP). The plasticity dynamics introduced by means of this linear approximation is not related to physiological processes [22], however, with this function we can find a fit which describes experimental results of eSTDP and iSTDP, as showed in References [18,19].

Figure 2a exhibits the eSTDP function for excitatory synapses, where the presynaptic neuron j and the postsynaptic neuron i are forced to spike at time t_j and t_i, respectively. There is a change in the synaptic weights $\Delta\varepsilon_{ij}$ due to the time difference between the spikes $\Delta t_{ij} = t_i - t_j$. The eSTDP function is given by [23]

$$\Delta\varepsilon_{ij} = \begin{cases} A_1 \exp(-\Delta t_{ij}/\tau_1), & \text{if } \Delta t_{ij} \geq 0 \\ -A_2 \exp(\Delta t_{ij}/\tau_2), & \text{if } \Delta t_{ij} < 0 \end{cases}, \tag{13}$$

where $A_1 = 1$, $A_2 = 0.5$, $\tau_1 = 1.8$ ms, and $\tau_2 = 6$ ms. The synaptic weights are updated according to equation (13), where $\varepsilon_{ij} \to \varepsilon_{ij} + 10^{-3}\Delta\varepsilon_{ij}$. The black line
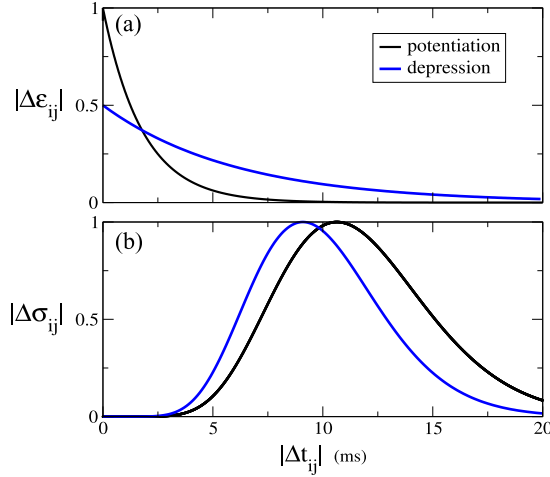
Fig. 2. Comparison between absolute values of potentiation (black curves) versus depression (blue curves) in synaptic weights. STDP function for (a) excitatory and (b) inhibitory synapses.

in Figure 2a shows the potentiation of excitatory synaptic weights for $\Delta t_{ij} \geq 0$ and the blue line the depression in synaptic weights for $\Delta t_{ij} < 0$.

In Figure 2b, we see the iSTDP function for inhibitory synapses. The weights are increased based on the following equation

$$\Delta\sigma_{ij} = \frac{g_0}{g_{\text{norm}}} \alpha^\beta |\Delta t_{ij}| \Delta t_{ij}{}^{\beta-1} \exp(-\alpha|\Delta t_{ij}|), \tag{14}$$

where $g_0 = 0.02$, $\beta = 10$, $\alpha = 0.94$ if $\Delta t_{ij} > 0$, $\alpha = 1.1$ if $\Delta t_{ij} < 0$ and $g_{\text{norm}} = \beta^\beta \exp(-\beta)$ [24,25]. The inhibitory synaptic weights are updated according to equation (14), where $\sigma_{ij} \to \sigma_{ij} + 10^{-3}\Delta\sigma_{ij}$.

In our neural network model, the time interval between spikes Δt_{ij} and the plasticity rules are calculated and applied every time the postsynaptic neuron i fires and can present different values depending on when the presynaptic neuron j had the last spike.

4 Synaptic weights and synchronization

In our simulations, aiming to understand the alterations in network connectivity, we consider a neuronal network with 100 Hodgkin–Huxley. This number of neurons was chosen to facilitate a visual analysis of the coupling matrices without loosing main dynamics properties. Our network has 80% of excitatory and 20% of inhibitory synapses according to anatomical estimates for the neocortex [26]. The neurons are initially globally coupled and the initial synaptic weights are normally distributed with mean 0.25 and standard deviation equal to 0.02. In this approach, to understand the impact of the delay in the system, we will consider that all the synapses have the same delay. In Figure 3, we see the coupling matrices, where the color bar represents the synaptic weights. The coupling matrix is separated into excitatory ($1 \leq i, j \leq 80$) and inhibitory ($81 \leq i, j \leq 100$) neurons. The excitatory neurons i are organized from the lowest frequency $i = 1$ to the highest frequency $i = 80$, and the inhibitory neurons from the lowest frequency $i = 81$ to the highest frequency $i = 100$.
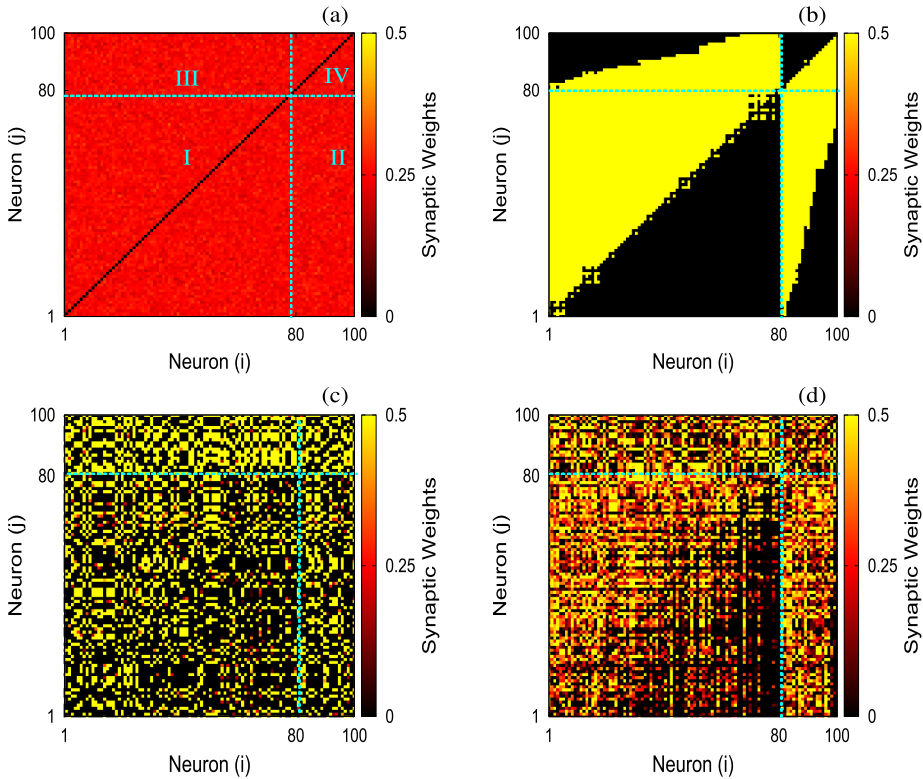
Fig. 3. Coupling matrices for excitatory and inhibitory neurons. Figure (a) shows the initial synaptic weights. We consider (b) $\tau = 0$ ms, (c) $\tau = 3$ ms and (d) $\tau = 6$ ms at 400 s. In four cases the color bar represents the synaptic weights.

Figure 3a exhibits the initial synaptic weights separated into 4 regions. In the regions I and II the synapses from the pre to the postsynaptic neurons are excitatory. The region III and IV have inhibitory synapses from the pre to postsynaptic neurons. For $\tau = 0$ ms, we observe in Figure 3b that the coupling matrix shows a triangular shape, due to the fact that the synapses become regulated by both the nature (excitatory or inhibitory) and the frequency of the presynaptic and postsynaptic neuron. A presynaptic excitatory (inhibitory) neuron with higher (lower) frequency enhances the synaptic strength if the postsynaptic excitatory (inhibitory) neuron has lower (higher) frequency. When the time delay is $\tau = 3$ ms and also $\tau = 6$ ms, as shown in Figures 3c and 3d, respectively, the coupling matrices have a non-trivial configuration of connections, presenting a greater agreement with real neuronal networks [27–29]. Therefore, the time delay has a significant influence on the synaptic weights in a neuronal network with plasticity, resulting in non-trivial configurations and synaptic weights with greater variability in their values if compared to the case without delay.

We analyze the time evolution of instantaneous average of excitatory $\varepsilon(t)$ and $\sigma(t)$ inhibitory coupling strengths for different time delay values. Without time delay $\tau = 0$ (Fig. 4a), ε (black line) has value greater than σ (red line). Whereas for $\tau = 3$ ms (Fig. 4b) and $\tau = 6$ ms (Fig. 4c) both ε and σ oscillate in the interval $[0.2; 0.3]$.

We study the effects of the time delay on the neuronal synchronization. To do
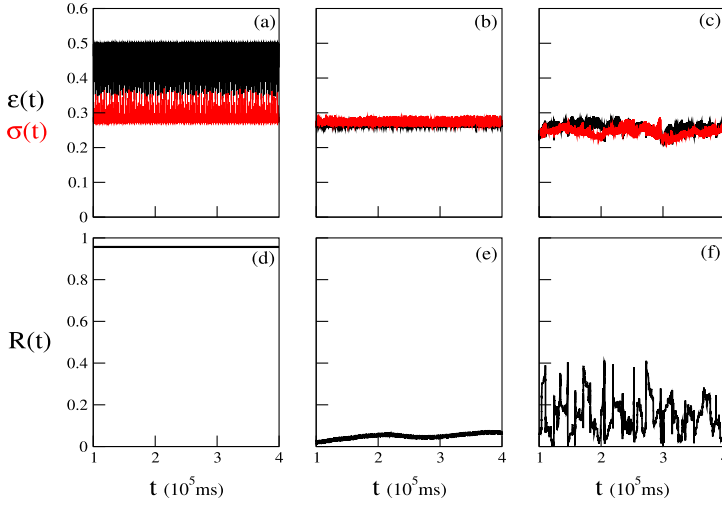
Fig. 4. In this set of figures we show the time evolution of $\varepsilon(t)$ (black line) and $\sigma(t)$ (red line) for (a) $\tau = 0$ ms, (b) $\tau = 3$ ms, and (c) $\tau = 6$ ms, as well as the time evolution of the Kuramoto's order parameter $R(t)$ for (d) $\tau = 0$ ms, (e) $\tau = 3$ ms, and (f) $\tau = 6$ ms.

that, we use the Kuramoto order parameter as diagnostic tool, that is given by [30]

$$R(t) = \left| \frac{1}{N} \sum_{j=1}^{N} \exp(i\phi_j(t)) \right|, \tag{15}$$

and the time averaged order parameter

$$\bar{R} = \frac{1}{t_{\mathrm{f}} - t_{\mathrm{i}}} \sum_{t_{\mathrm{i}}}^{t_{\mathrm{f}}} \left| \frac{1}{N} \sum_{j=1}^{N} \exp(i\phi_j(t)) \right|, \tag{16}$$

where $\phi_j(t)$ is the phase associated with the spikes,

$$\phi_j(t) = 2\pi m + 2\pi \frac{t - t_{j,m}}{t_{j,m+1} - t_{j,m}}, \tag{17}$$

where $t_{\mathrm{f}} - t_{\mathrm{i}}$ is the time window set to measure the phases, $t_{j,m}$ is the time when a spike m ($m = 0, 1, 2, \dots$) in the neuron j happens ($t_{j,m} < t < t_{j,m+1}$). The order parameter magnitude tends to unity when the network has a globally synchronized behavior. For uncorrelated spiking phases, the order parameter is nearly 0.

Figures 4d–4f exhibit the order parameter for (d) $\tau = 0$, (e) $\tau = 3$ ms, and (f) $\tau = 6$ ms. Our neuronal network does not exhibit complete synchronization due to the fact that the neurons are not identical. Nevertheless, for $R > 0.9$ the neuronal network shows strong synchronization behavior. In Figure 4d, we see a synchronous state for $\tau = 0$. There is no synchronization states observed for $\tau = 3$ ms and $\tau = 6$ ms, as shown in Figures 4e and 4f, respectively. This result shows that the delay is an important mechanism in the network dynamics in order to avoid synchronization.

In Figure 5a, we calculate the time averaged excitatory and inhibitory coupling strengths as a function of the time delay for 10 different initial conditions. The $\bar{\sigma}$
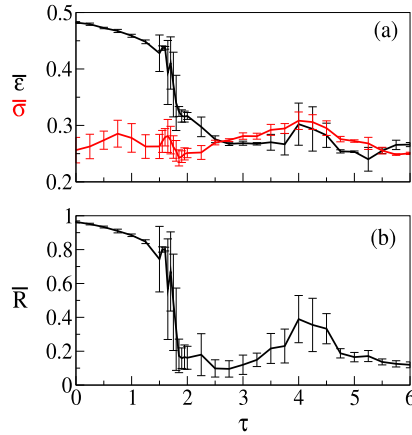
Fig. 5. (a) Average values of excitatory $\bar{\varepsilon}$, inhibitory $\bar{\sigma}$ synaptic weights, and (b) mean order parameter $\bar{R}$ as a function of synaptic time delay τ. The bars show the standard deviation from the mean values.

values present a small variation as the delay τ is increased. However, $\bar{\varepsilon}$ is more sensitive and for small delay values $\tau < 1.5$ ms we observe $\bar{\varepsilon} > \bar{\sigma}$ and the network is more excitable. As a result the neurons in the network are strongly synchronized (Fig. 5b). When we increase the delay for $\tau > 1.5$ ms the values of $\bar{\varepsilon}$ starts to decrease in a second-order-like transition. Simultaneously the order parameter $\bar{R}$ decreases showing its dependence with the excitatory coupling strength $\bar{\varepsilon}$. Finally, for $\tau > 2.5$ ms we observe that $\bar{\varepsilon}$ and $\bar{\sigma}$ oscillates in the interval $[0.2; 0.3]$ and the network are no longer synchronized. These results show us that synchronization in a neuronal network with plasticity and synaptic delay is closely linked to the intensity of excitatory couplings, i.e., the more excitable the network ($\bar{\varepsilon} > \bar{\sigma}$) the more synchronous the neurons will be.

5 Conclusion

We study a neural network with plasticity and synaptic delay, where we consider the Hodgkin–Huxley model as local dynamics. The Hodgkin–Huxley neuron is a mathematical model described by coupled differential equations that exhibits spiking dynamics. We build a network with an initial all-to-all topology and analyze the time evolution of the connectivity and synchronization.

We carry out simulations considering a coupling matrix with initial synaptic weights normally distributed. Without time delay, the coupling matrix evolves to a triangular shape, where the synapses become regulated by both the nature (excitatory) and the frequency of the presynaptic and postsynaptic neuron. A presynaptic excitatory (inhibitory) neuron with lower (higher) frequency enhances the synaptic strength if the postsynaptic excitatory (inhibitory) neuron has higher (lower) frequency. The coupling matrix exhibits non-trivial configuration when the time delay is increased.

We also show that the time delay plays an important role in the neural synchronization. Increasing the time delay, we verify that the time averaged excitatory coupling strength decrease and it becomes approximately equal to the averaged inhibitory coupling strength. As a consequence, this decrease suppresses the synchronous behavior of the neural network.

The results related to what is being shown in Figures 3c and 3d show that time delay induces a plastic brain with a non-trivial topology that promotes weak forms of synchronization, as it is to be expected in the brain. However, on the other hand, the brain is only sparsely connected. The evolved network has a higher rate between the actual connections and the number of neurons than this rate for the real brain. We believe that there could be 3 reasons for this which deserves further investigation. This non-sparsity of our evolved network could have been the consequence of some chosen parameters which are not optimally tunes to reproduce brain behavior. Another hypothesis could be that this non-sparsity is the result of our network being small, as compared to the real brain. Finally, it could be that the brain has a mechanism to constrain or eliminate connections in an attempt to optimize the costs associated to synapses.

References

1. A. Pascual-Leone, A. Amedi, F. Fregni, L.B. Merabet, Annu. Rev. Neurosci. **28**, 377 (2005)
2. B. Kolb, R. Gibb, J. Can. Acad. Child Adolesc. Psychiatry **20**, 265 (2011)
3. R.R. Borges, F.S. Borges, E.L. Lameu, A.M. Batista, K.C. Iarosz, I.L. Caldas, R.L. Viana, M.A.F. Sanjuán, Commun. Nonlinear Sci. Numer. Simul. **34**, 12 (2016)
4. R.R. Borges, F.S. Borges, E.L. Lameu, A.M. Batista, K.C. Iarosz, I.L. Caldas, C.G. Antonopoulos, M.S. Baptista, Neural Netw. **88**, 58 (2017)
5. R. Lestienne, Prog. Neurobiol. **65**, 545 (2001)
6. X.-J. Wang, Physiol. Rev. **90**, 1195 (2010)
7. B.C. Schwab, T. Heida, Y. Zhao, E. Marani, S.A. van Gils, R.J.A. van Wezel, Front. Syst. Neurosci. **7**, 60 (2013)
8. S. Boucetta, S. Chauvette, M. Bazhenov, I. Timofeev, Epilepsia **49**, 1925 (2008)
9. F.S. Borges, P.R. Protachevicz, E.L. Lameu, R.C. Bonetti, K.C. Iarosz, I.L. Caldas, M.S. Baptista, A.M. Batista, Neural Netw. **90**, 1 (2017)
10. E.L. Lameu, F.S. Borges, R.R. Borges, K.C. Iarosz, I.L. Caldas, A.M. Batista, R.L. Viana, J. Kurths, Chaos **26**, 043107 (2016)
11. E.R. Kandel, J.H. Schwartz, T.M. Jessel, *Principles of neural science* (Elsevier, Amsterdam, 1991)
12. Y. Hao, Y. Gong, L. Wang, X. Ma, C. Yang, Chaos Solids Fractals **44**, 260 (2011)
13. K. Lashley, Psychol. Bull. **30**, 237 (1923)
14. M.C. Diamond, D. Krech, M.R. Rosenzweig, J. Comput. Neurol. **123**, 111 (1964)
15. E.L. Bennett, M.C. Diamond, D. Krech, M.R. Rosenzweig, Science **146**, 610 (1964)
16. P. Bach-y-Rita, Acta Neurol. Scand. **43**, 417 (1967)
17. D.O. Hebb, *The organization of behavior* (Wiley, New York, 1949)
18. G.Q. Bi, M.M. Poo, J. Neurosci. **18**, 10464 (1998)
19. J.S. Haas, T. Nowotny, H.D.I. Abarbanel, J. Neurophysiol. **96**, 3305 (2006)
20. A.L. Hodgkin, A.F. Huxley, J. Physiol. **11**, 500 (1952)
21. S. Kalitzin, B.W. Van Dijk, H. Spekreijse, Biol. Cybern. **83**, 139 (2000)
22. A. Artola, S. Bröcher, W. Singer, Nature **347**, 69 (1990)
23. G.Q. Bi, M.M. Poo, Annu. Rev. Neurosci. **24**, 139 (2001)
24. S.S. Talathi, D.U. Hwang, W.L. Ditto, J. Comput. Neurosci. **25**, 262 (2008)
25. H.D.I. Abarbanel, S.S. Talathi, Phys. Rev. Lett. **96**, 148104 (2006)

26. C.R. Noback, N.L. Strominger, R.J. Demarest, D.A. Ruggiero, *The Human Nervous System: Structure and Function* (Humana Press, Totowa, NJ, 2005)
27. S. Rieubland, A. Roth, M. Häusser, Neuron **4**, 913 (2014)
28. S. Yu, D. Huang, W. Singer, D. Nikolić, Cerab. Cortex **18**, 2891 (2008)
29. P. Bonifazi, M. Goldin, M.A. Picardo, I. Jorquera, A. Cattani, G. Bianconi, A. Represa, Y. Ben-Ari, R. Cossart, Science **326**, 1419 (2009)
30. Y. Kuramoto, *Chemical oscillations, waves and turbulence* (Spring-Verlag, Berlin, 1984)